JOURNAL OF VIROLOGY, July 2006, p. 6387–6398 Vol. 80, No. 13
0022-538X/06/$08.00+0 doi:10.1128/JVI.00352-06

Role of Pseudorabies Virus Us3 Protein Kinase during Neuronal Infection

L. M. Olsen,[1] T. H. Ch'ng,[1] J. P. Card,[2] and L. W. Enquist[1]*

Department of Molecular Biology, Princeton University, Princeton, New Jersey 08544,[1] and Departments of Neuroscience and Psychiatry, University of Pittsburgh, Pittsburgh, Pennsylvania 15260[2]

Received 20 February 2006/Accepted 11 April 2006

The pseudorabies virus (PRV) Us3 gene is conserved among the alphaherpesviruses and encodes a serine/threonine protein kinase that is not required for growth in standard cell lines. In this report, we used a compartmented culture system to investigate the role of PRV Us3 in viral replication in neurons, in spread from neurons to PK15 cells, and in axon-mediated spread of infection. We also examined the role of Us3 in neuroinvasion and virulence in rodents. Us3 null mutants produce about 10-fold less infectious virus from neurons than wild-type virus and have no discernible phenotypes for axonal targeting of viral components in cultured peripheral nervous system neurons. After eye infection in rodents, Us3 null mutants were slightly attenuated for virulence, with a delayed onset of symptoms compared to the wild type or a Us3 null revertant. While initially delayed, the symptoms increased in severity until they approximated those of the wild-type virus. Us3 null mutants were neuroinvasive, spreading in both efferent and afferent circuits innervating eye tissues.

The alphaherpesviruses, such as the human pathogens herpes simplex virus types 1 and 2 (HSV-1; HSV-2), varicella-zoster virus, and the agricultural-animal pathogens, such as pseudorabies virus (PRV), bovine herpesvirus type 1, and Marek's disease virus, are pantropic but are capable of invading the peripheral nervous systems (PNS) and central nervous systems (CNS) of susceptible animals (18, 34, 39). The infection of polarized cells, such as epithelial cells and neurons, plays a central role in the alphaherpesvirus life cycle. For example, primary infection usually occurs in mucosal epithelial cells, but after replication and release of virions at the basolateral surface, infection readily spreads to underlying nerve terminals of neurons of the PNS. The encapsidated viral genome then spreads directionally inside axons via microtubules to the cell bodies of sensory and autonomic ganglia. After entering the nucleus, the viral DNA is transcribed, and the neuron may experience a productive or latent infection. Most infections of natural hosts result in latent infections. After reactivation from a latent infection in PNS neurons, viral genomes move into axons and reverse their original direction by spreading back to the periphery, where upon release, progeny virions can infect epithelial cells and spread to other hosts. In rare cases after infection of the natural host, primary infection results in systemic spread of infection and occasional invasion of the CNS. When nonnatural hosts are infected, the outcome is reversed: latent infections and survival are rare, while rapid death and invasion of the CNS are common (3, 5, 25, 35).

It is well established for PRV that infection of nonnatural hosts, such as dogs, cattle, and rodents, by virulent strains causes a peripheral neuropathy characterized by violent pruritus (the mad itch) and rapid demise of the animal (51). Certain live, attenuated vaccine strains (notably the well-studied Bartha strain of PRV) have markedly reduced virulence in nonnatural hosts so that peripheral lesions and pruritus are absent and the animals survive longer (4, 5, 29). Unlike virulent virus infection, where animals die rapidly, often before substantial spread to the CNS can be observed, these attenuated strains are remarkably neuroinvasive and spread readily in the retrograde direction through chains of synaptically connected neurons in the CNS. Ultimately, the animals do succumb to infection, but only after extensive CNS infection. Accordingly, attenuated strains, such as Bartha, have been successfully exploited to trace the neural circuitry of the PNS and CNS in diverse model organisms (17, 27, 46).

The directional spread of PRV infection from polarized epithelial cells to axons of the PNS, followed by axonal transport to and from neuron cell bodies, is understood only in principle. The molecular mechanisms involved in entry, movement, and sorting of virion components in neurons remain to be characterized in detail. Certainly, efficient use and regulation of neuronal axonal targeting and transport mechanisms are essential for axonal entry and egress (41, 44). It has been established that HSV-1 capsid transport in nonneuronal cells is mediated by cellular microtubules and kinesin and dynein motor proteins (15, 16, 45). The inner tegument proteins of the HSV virion play key roles in such microtubule-based motion (52). Confocal imaging of living neurons infected with recombinant viruses expressing fluorescently tagged proteins has provided some important clues to the cell biology of viral axonal transport. For example, the kinetics of PRV capsid movement in cultured sensory neurons revealed that both entry and egress occur by fast axonal transport via microtubules, but each process has distinct kinetics and specific sets of associated tegument proteins (30, 31). However, the precise compositions of uncoated viral particles after axonal entry and of newly forming progeny virions during egress from axon terminals remain to be established (12, 23, 28).

A key question centers on how the direction of transport is established in axons (toward the cell body during entry and away from the cell body during egress) (19). The alphaherpesvirus virion tegument layer contains at least two protein kinases (Us3 and UL13) (22) that have been proposed to play roles in establishing directional movement of encapsidated genomes by phosphorylating key motor components so that the

* Corresponding author. Mailing address: Department of Molecular Biology, Princeton University, Princeton, New Jersey 08544. Phone: (609) 258-2415. Fax: (609) 258-1035. E-mail: lenquist@princeton.edu.

TABLE 1. Virus strains used in this study

Virus	Description	Reference
PRV Becker	Wild type; parental strain	Laboratory strain
PRV 813	Us3 null; Us3ns; nonsense mutation	This work
PRV 813R	Revertant of PRV 813; Us3R	This work
PRV 180	PRV Becker expressing mRFP-VP26, red fluorescent capsid; (red-capsid virus)	12
PRV 823	Recombinant between PRV 813 and PRV 180; Us3 null virus expressing mRFP-VP26 (red capsid/Us3 null)	This work
PRV 182	PRV Becker expressing mRFP-VP26 and eGFP-VP22; red fluorescent capsid; green tegument protein; (dual-color virus)	12
PRV 833	Recombinant between PRV 813 and PRV 182; Us3 null virus expressing mRFP-VP26 and eGFP-VP22; (dual-color Us3 null virus)	This work

dynein motors are active during entry and the kinesin motors are active during egress (41, 43). In this report, we have compared neuronal infections in vivo and in vitro using PRV Us3 null mutants and the wild-type or revertant viruses.

In the alphaherpesviruses, the Us3 protein kinase has been associated with a variety of virus-cell interactions. For example, PRV Us3 null mutants exhibit reduced plaque size in some cell types, particularly those of epithelial origin (6, 14). Us3 also plays a role in modulating apoptosis, actin stress fiber breakdown, and de-envelopment from the perinuclear space during nuclear egress (21, 49). The neurovirulence of alphaherpesviruses in the absence of Us3 has been examined primarily via intracranial injections of mice. The 50% lethal dose of HSV-1 Us3 mutants in this model was reduced by 4 orders of magnitude, whereas HSV-2 Us3 mutants exhibited only moderate defects in viral replication and 50% lethal dose (10-fold) (26, 33, 37). Asano and colleagues studied the role of Us3 in the spread of HSV-2 within the brain after mouse corneal infections (1). While the HSV-2 Us3 null mutant spread from the cornea to the trigeminal ganglion via primary afferent neurons, subsequent viral spread was restricted compared to wild-type virus and correlated with an increased incidence of apoptotic cell death. The effects of Us3-deficient PRV have recently been investigated using porcine trigeminal ganglion cells (20, 21). When these PNS neurons are productively infected by wild-type or Us3-deficient PRV, they become resistant to PRV-induced apoptosis compared to the responses of other cell types. In these studies, despite antiapoptotic activity of Us3 in swine kidney cells, the absence of Us3 had no effect on resistance to cell death or suppression of apoptosis in these trigeminal ganglion cells.

MATERIALS AND METHODS

Virus strains and cells. PRV Becker (a virulent laboratory strain) was used as the wild-type virus in all of the experiments (Table 1). All PRV strains and mutants were propagated in PK15 cells, a transformed, adherent epithelial pig kidney cell line (ATCC number CCL-33). PK15 cells were grown in Dulbecco's modified Eagle's medium (DMEM) supplemented with 10% fetal bovine serum (FBS), and viral infections were performed in DMEM supplemented with 2% FBS. PC12 cells were grown and differentiated as previously outlined (9). Nerve growth factor (NGF)-differentiated PC12 cells used in all experiments were maintained in RPMI medium supplemented with 1% horse serum and NGF.

Plasmids. Us3 subclones pLO12 (pGEM vector with a 1.7-kb fragment of the PRV Becker Us region containing the Us3 coding region [both major and minor], as well as a fragment of the glycoprotein G [gG] open reading frame) and pLO14 (with a 1-kb coding region for kanamycin resistance from pUC4K inserted into pLO12) were used. In the latter construction, 1.1 kb of Us3 sequences are lost and replaced with a kanamycin resistance cassette.

Site-directed mutagenesis (QuickChange). pLO4 is a Quickchange vector (psp72) digested with BamHI/EcoRI and religated to include a linker containing RsrII/BlpI/DraII sites. The linker was created by annealing the following primers (heated to 80°C for 5 min and then cooled to room temperature for 1 h): 5′GATCCCGGACCGATAGCTCAGCTTACACGGTGTGG3′ and 5′AATTC CACACCGTGTAAGGTCCGATATCGGTCCGG3′. pLO10 is a 0.5-kb DraII/BlpI fragment (Us3) ligated into BlpI/DraIII-digested pLO4. This plasmid was used as a template for Us3 null site-directed mutagenesis. pLO18 was constructed by ligating a 2.5-kb insert produced by partial PvuII digestion of pLO14 (Us3::Kan) into a PvuII-digested pGS284 allelic-exchange vector. pLO20 was

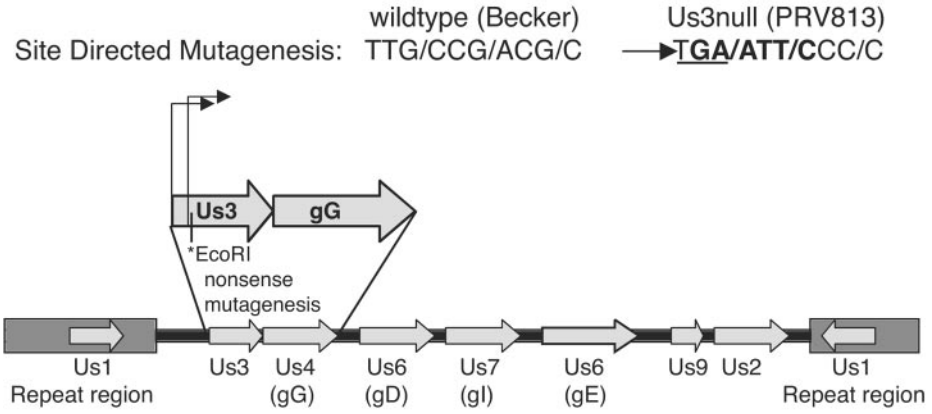

FIG. 1. Site-directed mutagenesis of Us3. Us3 is located in the unique short region of the PRV genome and has two transcriptional start sites. PRV 813, a Us3 null mutant, was constructed through site-directed mutagenesis that inserted a nonsense mutation (underlined) just downstream of the second transcriptional start site. Mutagenesis was marked with the concomitant insertion of a novel EcoRI restriction site (bold) and resulted in the elimination of Us3 protein production.

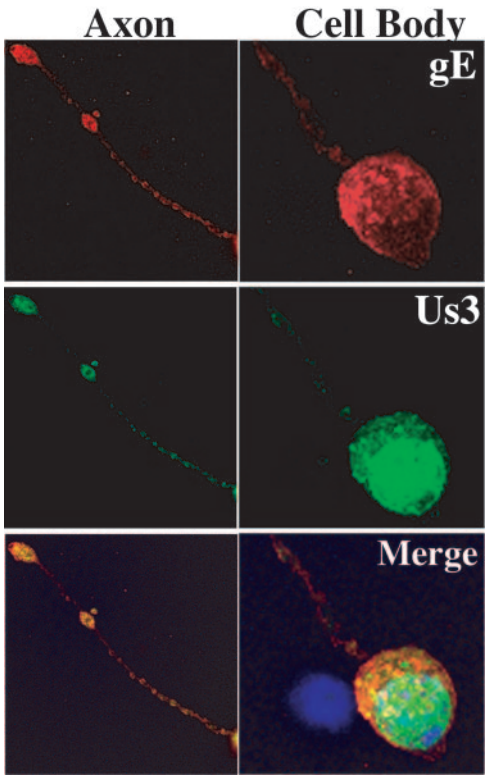

FIG. 2. Localization of Us3 protein in PRV Becker-infected differentiated PC12 cells at 8 h postinfection. Samples were fixed with 2% paraformaldehyde and stained for Us3 (green), DNA (blue), and gE (red). Us3 localization was primarily perinuclear in the cell bodies and punctate in the axons.

constructed by using PCR from the pLO10 template. pLO24 was constructed by ligating the 0.5-kb DraII/BlpI fragment of pLO20 into DRAII/Blp1-digested pLO16.

Primers. As shown in Fig. 1, the primer Us3ns (5′-ATCTCGTCGGGGATT CCGGGAATTCACATTGTTGCTGCGTGCGAGC3′) was used for the introduction of a TAG nonsense mutation and an EcoRI site downstream of the major start methionine.

Antisera. A monoclonal antibody specific for Us3 was directed against a fusion protein produced in *Escherichia coli* in which the C-terminal 158 amino acids of Us3 were fused to glutathione-*S*-transferase protein (pLO2). Mice were immunized with purified protein, and hybridomas 7H10-21 and 8F8-6 were selected for further propagation. Both monoclonal antibodies were immunoglobulin G1(κ) isotypes. Hybridoma 7H10-21 supernatant was concentrated by ammonium sulfate precipitation and clarified with uninfected PK15 cell lysate.

Construction of PRV Us3 mutants (Fig. 1). The BAC infectious clone pBecker 3 was used for mutant construction essentially as described by Smith and Enquist (42).

Construction of Us3::KAN and Us3 nonsense mutants. The plasmid PRV800/pLO800 contains a kanamycin resistance cassette in place of the deleted Us3 open reading frame derived from pLO18. PRV 800 (Us3::KAN) was constructed by allelic exchange between GS564 and pLO18 and confirmed by Southern blotting. A nonsense mutant allele of Us3 called PRV 813 was constructed by allelic exchange between pLO24 and pLO800. Both mutants formed small plaques on Madin-Darby bovine kidney (MDBK) cells. Accordingly, stocks of these two Us3 null mutants were always screened for the presence of large-plaque revertants that could obfuscate subsequent assays.

Construction of double and triple mutants carrying a Us3 null allele and also expressing mRFP-VP26 or eGFP-VP22 fusion proteins. Double mutants were constructed by in vivo recombination after mixed infection of PK15 cells (Table 1). PRV 180 (which expresses an mRFP-VP26 fusion protein [mRFP is monomeric red fluorescent protein]) that is assembled into capsids or PRV 182 (which expresses both mRFP-VP26 and eGFP-VP22 fusion proteins [eGFP is enhanced green fluorescent protein]) were crossed with PRV 813 (multiplicity of infection [for each virus], 5). The use of mRFP in PRV infections has been described by Banfield and colleagues (2). PRV 180 and PRV 182 have been described previously (12). Recombinants were identified initially by their small plaque size on MDBK cells and by fluorescence microscopy to assess expression of mRFP or eGFP. Five rounds of plaque picking and amplification on PK15 cells were performed to purify double and triple mutants to homogeneity.

Viral infections. Protocols for viral infection of neurons have been described by Ch'ng and Enquist (11). All PRV infections of neuron cultures were carried

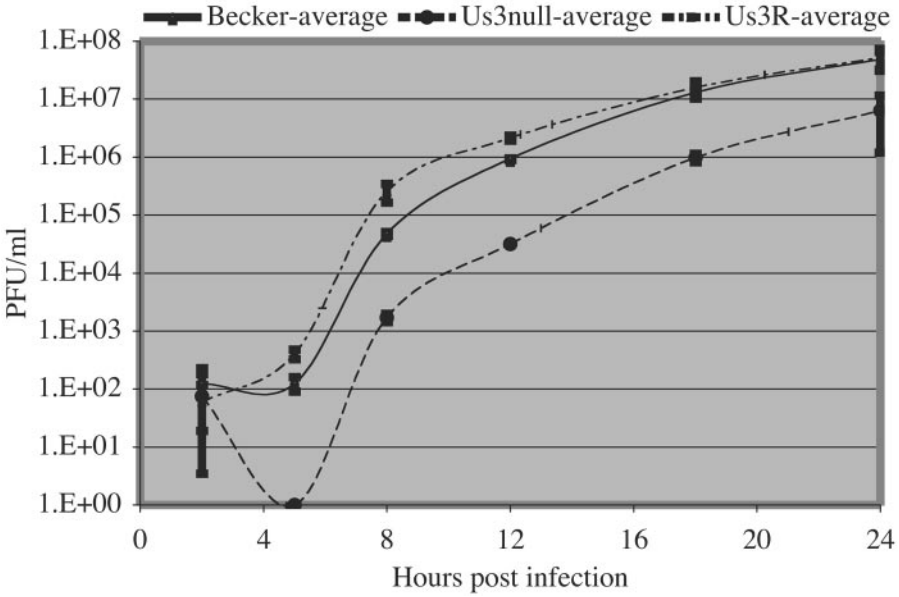

FIG. 3. Single-step growth analysis of Us3 null virus on differentiated PC12 cells. The presence of infectious virus (PFU/ml) was monitored at 2, 5, 8, 12, 18, and 24 h postinfection. Compared to wild-type (PRV Becker) and Us3 null revertant (PRV 813R; Us3R) virus, the Us3 null infection (PRV 813) exhibited an increased eclipse period during which no infectious virus was detectable and grew to 10-fold-lower titers by 24 h postinfection.

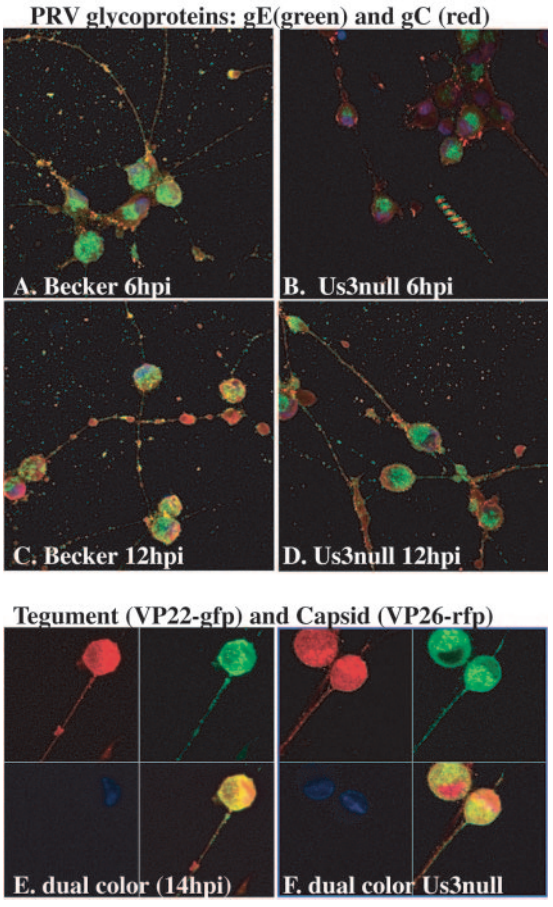

FIG. 4. Axonal localization of virion components in differentiated PC12 cells during PRV infection. Glycoproteins (gE and gC) and tegument (VP22) and capsid (VP26) proteins are localized to the axons of PC12 cells during PRV Becker and Us3 null infections (PRV 813). (A to D) Time course of viral-glycoprotein production in differentiated PC12 cells. Us3 null-infected cells exhibited reduced expression of glycoproteins gE and gC early (6 h) in infection but maintained wild-type localization within the cell body and axons. Confocal images were obtained from *z*-stacked images. The striped pattern observed in the lower right corner of panel B was produced by stacking serial images that contained floating debris. Dual-color PRV 182 (E) and dual-color PRV 833 Us3 null (F) virus infections of PC12 cells demonstrate efficient axonal localization of VP22 (green) and capsid (red) proteins in the presence and absence of Us3 expression.

out with sufficient virus inoculum to infect essentially all neurons in the dish unless otherwise stated. Briefly, neurons were cultured on Delta TPG dishes (Bioptechs) and grown to maturity for approximately 2 to 3 weeks prior to any experiment. The viral inoculum was diluted in 2% FBS in DMEM (Invitrogen) and overlaid on the neuronal culture for 1 h in a humidified 37°C incubator. After 1 h, the viral inoculum was removed and replaced with neuron medium. Samples were fixed and processed for immunofluorescence.

Single-step growth analysis. PC12 cells were grown and infected as described by Ch'ng et al. (9). The cells were infected for 1 h at a multiplicity of infection of 20 in 0.5 ml of RPMI-1% horse serum. The inoculum was removed, and the cells were treated for 1 min with citrate wash, washed two times with RPMI, and covered with 1 ml of conditioned medium for the duration of the experiment. Cells were harvested at 2, 5, 8, 12, 18, and 24 h postinfection and stored at −70°C. The cells were freeze-thawed three times, sonicated, and titered on PK15 cells.

Immunofluorescence sample preparation. Samples were fixed with 2% paraformaldehyde in phosphate-buffered saline (PBS) for 10 min, permeabilized in a 0.2% Triton X-100–PBS solution for 15 min, blocked in a 10% horse serum-1% bovine serum albumen (BSA) solution in PBS for 1 h, and stained by diluting primary or secondary antibodies in a 1% bovine serum albumen solution in PBS for 1 h at room temperature. Coverslips were rinsed two times with distilled water and then mounted using AquaPoly/Mount (Polysciences Inc.). In some cases, DNA was stained with Hoechst 33342 (H1399; Molecular Probes) according to standard protocols, and images were collected with a Zeiss LSM510 scanning confocal microscope using a 63× oil objective as described previously (10).

Live-cell confocal microscopy. Cells for live imaging were grown on coated Delta TPG dishes (Bioptechs), infected, and directly imaged in a 50:50 mix of DMEM and F-12 (without phenol red) medium. Neurons were infected and incubated at 37°C. The cells were maintained in a 5% CO_2, 37°C heated chamber (Live Cell Systems) using a Perkin-Elmer R30 spinning-disc confocal microscope. Image analysis was conducted with Perkin-Elmer ImageView software.

Compartmented culture system. This system has been described previously (11). Briefly, primary dissociated superior cervical ganglion (SCG) neurons from embryonic rats were cultured in one of the side compartments (the S [soma] compartment) in a trichamber Teflon ring. This ring was sealed onto a 35-mm tissue culture dish with a thin continuous strip of silicone grease applied evenly on the surface of the ring. Once the neurons matured, the axons penetrated underneath the silicone grease barrier to emerge in the other side compartment (the N [neurite] compartment), where other cell types could be cocultured on top of the axons. In neuron-to-cell spread studies, PK15 cells cocultured with axons in the N compartment could be harvested and titered to detect the presence of infectious particles. Similarly, in axon-mediated spread of infection, the neuron cell bodies in the S compartment were harvested and titered 24 h postinfection. The physical separation between sites of infection and viral replication allowed the specific infection of neurite extensions or soma and subsequent analysis of retrograde axonal transport (neurite to cell body) during entry or anterograde transport (cell body-to-neurite extensions) during egress. The presence of mature infectious particles, harvested from the initially uninfected chamber at 24 h postinfection, measured the extent of axonal transport and egress. This system has been demonstrated to recapitulate the in vivo spread phenotypes of gE, gI, and Us9 mutants (10; our unpublished data).

Animal infections. The rat eye infection model has been previously described (8, 39). In this report, 11 animals received an intravitreal injection of either the Us3 null mutant ($n = 7$; titer = 5.5×10^8 PFU/ml), the revertant ($n = 2$; titer = 4.0×10^9 PFU/ml), or PRV Becker ($n = 2$; titer = 4.5×10^9 PFU/ml). Virus was injected into the vitreous body of one eye using a 10-μl Hamilton microliter syringe. Two animals in the control groups (one each of Becker and the revertant) were injected with 4 μl of virus. All of the other animals were injected with 2 μl of virus. Virus was injected slowly over a 5-min period, and the syringe needle remained in the globe of the eye for 5 min after virus injection to reduce leakage into the orbit. The animals were anesthetized and perfused transcardially with buffered aldehyde solutions. The brain and spinal cord were sectioned at 35 μm, and infected neurons were localized immunohistochemically using a rabbit polyclonal antiserum (Rb-133) raised against acetone-inactivated virus. The specificity of this antiserum for central localization of PRV-infected neurons was established previously (8).

RESULTS

Single-step growth in PC12 cells. Differentiated PC12 cells provided a facile cell line to establish neuronal phenotypes of Us3 mutants. These rat pheochromocytoma cells can be differentiated into neuron-like cells in the presence of NGF. Upon differentiation, the cells undergo morphogenic changes, cease to replicate, and acquire many of the properties of sympathetic neurons (24). In infected epithelial cells, Us3 localizes to the nucleus early in infection but also exhibits diffuse cytoplasmic and faint plasma membrane staining late in infection. As demonstrated in Fig. 2, Us3 localizes predominantly to the PC12 nucleus, with distinct cytoplasmic puncta, but is also present in the axons (these neurites stain with axon-specific markers and not dendrite-specific markers (48). gE colocalizes with Us3 in axons, primarily in the varicosities along the axons, as well as at the terminals (Fig. 2).

The single-step growth curves of the parental PRV Becker strain, PRV 813 (Us3 null), and PRV 813R (Us3 null rever-

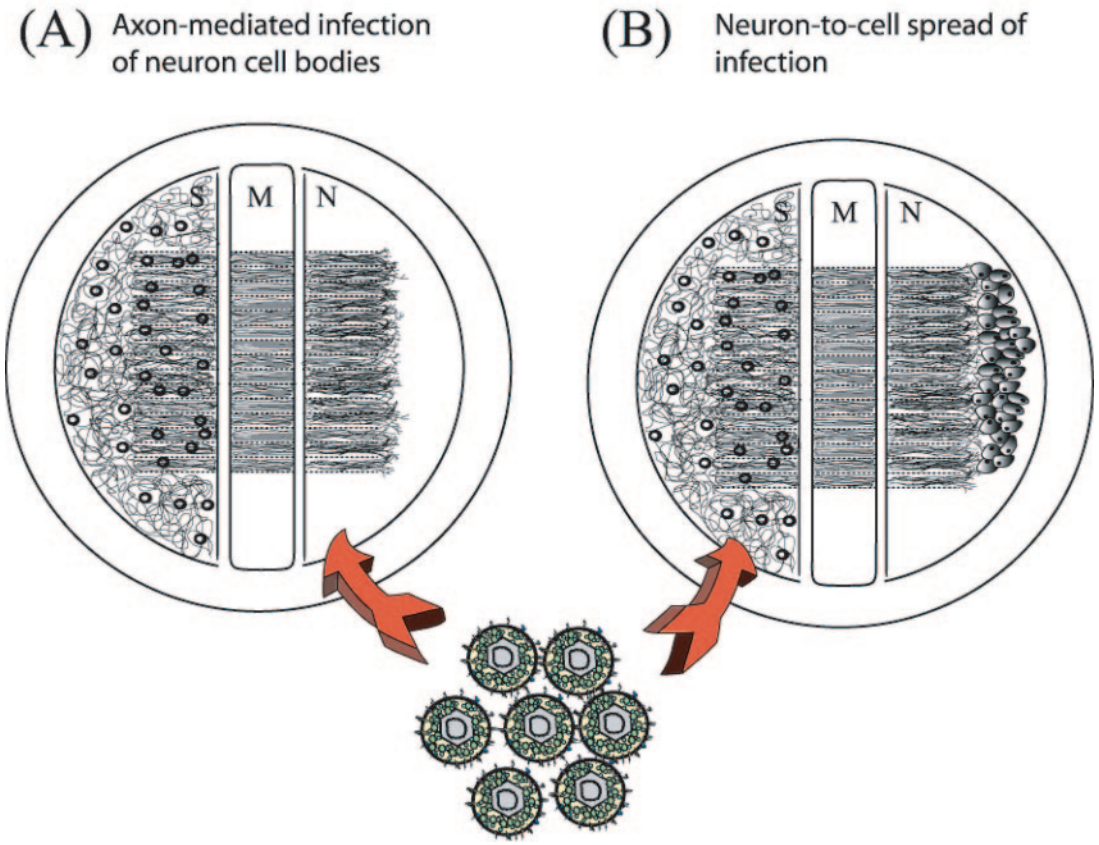

FIG. 5. Trichamber compartment culture system. The experimental apparatus used to determine the effects of Us3 null on retrograde and anterograde transport within axons has been previously described (11). For axon-mediated infection of neuron cell bodies (A), infection was initiated in the N compartment. As infection proceeded, cell bodies and extracellular medium from the S compartment were collected and titered. The middle compartment (M) was filled with media and methocel to act as a diffusion barrier. For determination of the neuron-to-cell spread of infection (B), detector PK15 cells were plated in the N compartment after axons had penetrated the N compartment. Infection was initiated in the S compartment, and after 24 h, the infection spread from axons to PK15 cells. Medium from the N compartment was harvested and titered.

tant) are depicted in Fig. 3. The kinetics of virus production in PC12 cells were no different than those described previously for other cell lines. Plaque-forming virus first appeared for PRV Becker and the Us3 null revertant virus at 5 h postinfection and accumulated to about 10^8 PFU/ml by 24 h. Also, consistent with results in other cell types, infection by the Us3 null mutant exhibited a longer eclipse phase, with infectious-virus production evident only after 8 h. The final yield of infectious virus for Us3 null infection was 10-fold lower than that produced by PRV Becker infection, again consistent with previous results in other cell culture systems (6, 13, 14).

Protein localization in infected PC12 cells. We determined the times of appearance, abundances, and axonal localization of selected viral proteins after infection of PC12 cells by various PRV mutants. Viral-protein expression was monitored by direct fluorescence or immunofluorescence using confocal microscopy. We examined viral-glycoprotein production in PRV Becker- and Us3 null mutant-infected cells at early (6 h) and late (12 h) times after infection (Fig. 4A to D). The amount of detectable glycoprotein production in Us3 null mutant-infected cells was reduced at 6 h compared to wild-type-infected PC12 cells. Western blot analyses and immunofluorescence studies of nonneuronal cell cultures indicate this reduction in protein production is not specific to neuronal cells and correlates with delayed and reduced production of virons (data not shown). However, in regard to protein localization within PC12 cells, at both early and late times in infection, glycoproteins in Us3 null- and Becker-infected cells exhibit similar distribution patterns, with gE and gC localized to Golgi-like compartments and the plasma membrane, respectively, and both glycoproteins are present in distinct puncta in axons by 12 h. We also visualized simultaneously the axonal localization of fluorescent tegument and capsid proteins using PRV 182 (eGFP-VP22/mRFP-VP26) (Fig. 4E) and PRV 833 (Us3 null eGFP-VP22/mRFP-VP26) (Fig. 4F). Late in infection (14 h), both eGFP-VP22 and mRFP-VP26 proteins are easily detectable in cell bodies and axons in the presence or absence of Us3. These analyses confirm that Us3 is not required for targeting of virion components to neuronal compartments.

Axonal transport in primary neuronal cultures. We next looked for directional-spread phenotypes of PRV Us3 null mutants in primary cultures of rat PNS neurons. Within neurons, the movement of cargo from the cell bodies to the axonal terminus requires the action of kinesin motors moving from the minus to the plus ends of microtubules (anterograde transport). Movement of cargo from axon termini to cell bodies,

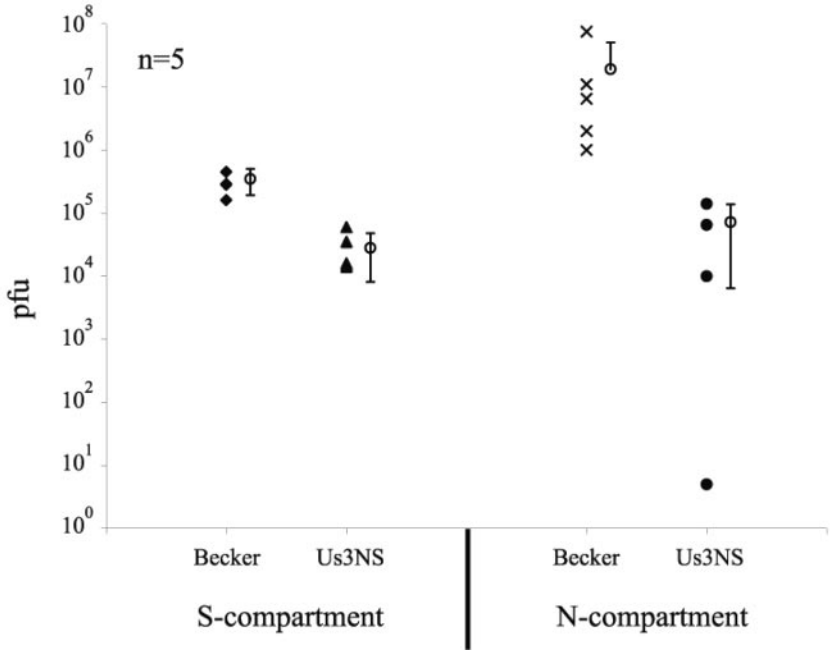

FIG. 6. Neuron-to-cell spread of infection. When cell bodies were infected in the S compartment, encapsidated genomes moved to varicosities and terminals in the N compartment and spread to the PK15 detector cells. The presence of infectious virus in the N compartment at 24 h was evidence for axon-mediated spread of infection to the detector cells. Titers of the contents of the S compartment (left) and the N compartment (right) at 24 h are indicated. Each open circle with error bars represents the average value for the five adjacent sets of data points.

from the plus to minus ends of microtubules (retrograde transport), requires dynein motors. During PRV infection, axonal targeting of encapsidated genomes and virion components, followed by anterograde transport, is essential for subsequent transsynaptic spread to postsynaptic neurons or other cells. Similarly, when virions bind to axon terminals at sites of entry, uncoated capsids with associated tegument proteins require retrograde transport to move to the cell body.

We used the trichamber compartmented system of Ch'ng and Enquist to analyze retrograde and anterograde movement of the encapsidated genomes of Us3-deficient mutants in axons after infection of primary rat neurons (11). The experimental setups for anterograde and retrograde infections are illustrated in Fig. 5A and B. Infection of SCG neurons with PRV Becker and Us3 null virus resulted in growth phenotypes similar to those observed after infection of PC12 cells (Fig. 3 and data not shown).

To detect the spread of infection from neuron cell bodies to distal axon terminals and then to nonneuronal cells, we plated PK15 detector cells in the N compartment (see Materials and Methods). The presence of infected detector cells reflects anterograde transport in axons from cell bodies to axon terminals, as well as subsequent spread of infection across the neuron-PK15 cell junction. Twenty-four hours after the cell bodies in the S compartment were infected, the media of both S and N compartments were harvested and titered. As demonstrated in Fig. 6, the yield of infectious virus in the S compartment after Us3 null infections was reduced 10-fold (Fig. 6). Neuron-to-PK15 cell spread was detectable in both PRV Becker and Us3 null infections, but the yield of Us3 null virions in the N compartment was reduced by 100-fold compared to the yield for PRV Becker (Fig. 6). These data indicate that Us3 may have a role in neuron-to-cell spread. However, Us3 null mutants exhibited a 10-fold reduction in both PC12 (Fig. 3) and PK15 (data not shown) cells. Therefore, a qualitative effect of Us3 on neuron-to-cell spread within this system is difficult to demonstrate, and these data may reflect only the reduced production of infectious virions from cell bodies. The data indicate that Us3 is not absolutely required for axon-mediated spread to PK15 cells.

Axon-mediated infection of neuronal-cell bodies. In this paradigm, infection is initiated at the exposed axons in the N compartment, and the yield of infectious virus produced by cell bodies in the S compartment is assayed. When the S compartment was titered at 14 h after axon infection by the Us3 null mutant, no infectious particles were detected (Fig. 7A). However, at 24 h after axon infection by the Us3 null mutants, the titer in the S compartment was reduced 10-fold compared to similar infections by PRV Becker and the Us3 null revertant (Fig. 7B). This modest reduction in titer corresponds to the yield obtained for Us3 mutants in a variety of cells. This experiment indicates that Us3 is not essential for retrograde transport of entering infectious particles from distal neurites to the cell bodies. One explanation for the difference in titers at 14 and 24 h is that axon-mediated infection of cell bodies by the Us3 null mutant is delayed compared to the wild-type virus. To test this idea, we repeated the studies and examined the production of an early viral protein (gE) in the cell bodies by immunofluorescence. By 14 h after infection, the number of infected cells was markedly reduced for the Us3 null mutant compared to PRV Becker. More than 80% of the cell bodies were positive for gE after PRV Becker infection, while less

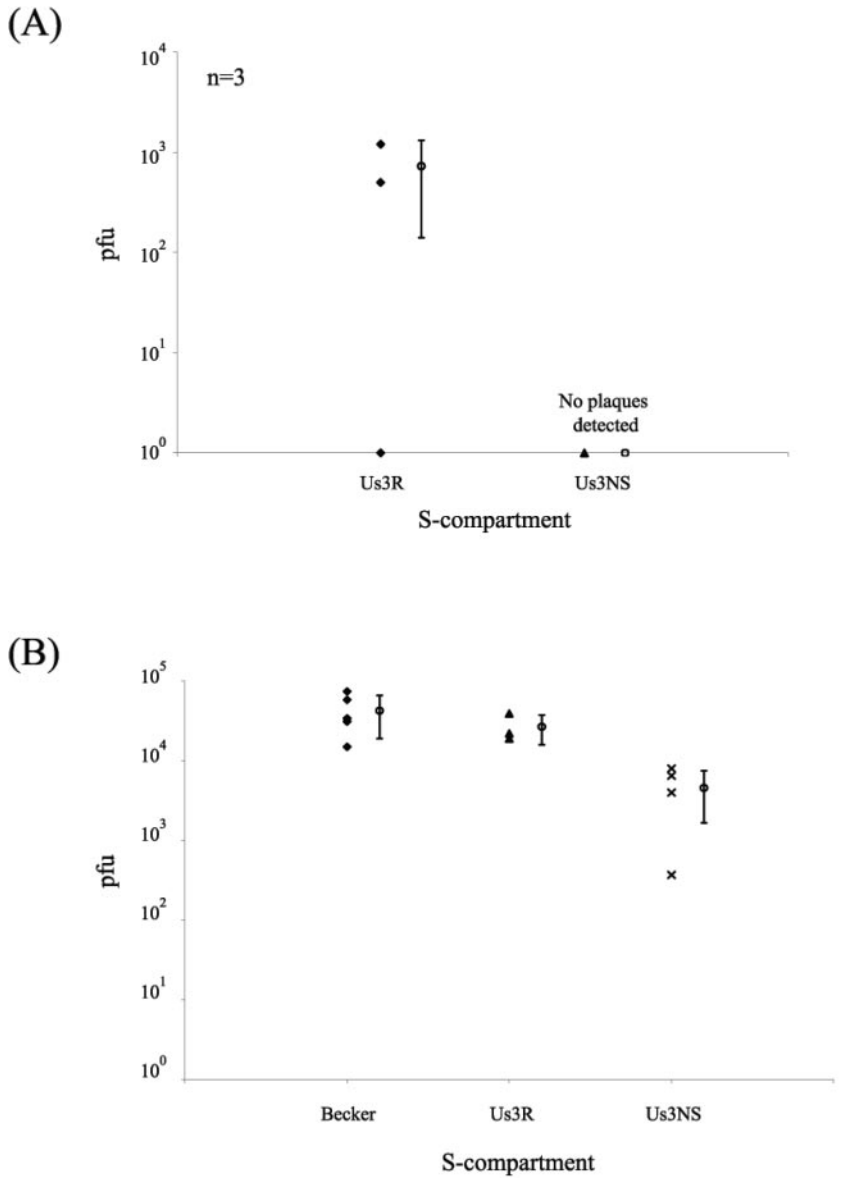

FIG. 7. Axon-mediated spread of infection to neuronal cell bodies. When neurites in the N compartment were infected, infectious-virus production in the S compartment indicated successful intra-axonal transport of entering particles to cell bodies, followed by productive replication. Titers of the S compartment at 14 h (A) and 24 h (B) are given. PRV Becker, PRV 813 (Us3 null), and PRV 813R (Us3 null revertant; Us3R) all spread to the cell bodies and replicated, but infectious virus in Us3 null-infected cells could not be detected until 24 h (B). For panel B, $n = 5$.

than 10% of the cell bodies were positive for gE after Us3 null mutant infection (Fig. 8A to D). By 24 h, this striking difference disappeared, and the number of gE-positive, Us3 null mutant-infected cell bodies became equivalent to that of PRV Becker at 14 h postinfection (Fig. 8E and F). Infections with the Us3 revertant virus were similar to those done with PRV Becker (data not shown). These data suggest two possible roles for Us3 in the axon-mediated spread of infection. One is that Us3 is required for efficient entry and subsequent transport toward the cell body in axons. Another is that Us3 is required for efficient spread of infection among cell bodies in the S compartment. Because this assay does not distinguish between primary infection initiated at the neurites and subsequent infection via cell-to-cell spread among cell bodies, these data cannot distinguish between these two possible roles for Us3.

Directional spread of PRV infection in animals. The rat eye infection model is useful to investigate both circuit-specific directional neuroinvasion and virulence phenotypes (reviewed in reference 39). Virulence analyses were limited to qualitative observations of time to onset of symptoms, severity of symptoms, and time to imminent death. Animals were sacrificed prior to death, the brains were removed, and tissue sections were analyzed for viral antigen to determine the extent of neuroinvasiveness. PRV Becker is a virulent wild-type isolate that causes death in rats by approximately 68 h after intraocular injection (7, 50). Rather than measure actual time of

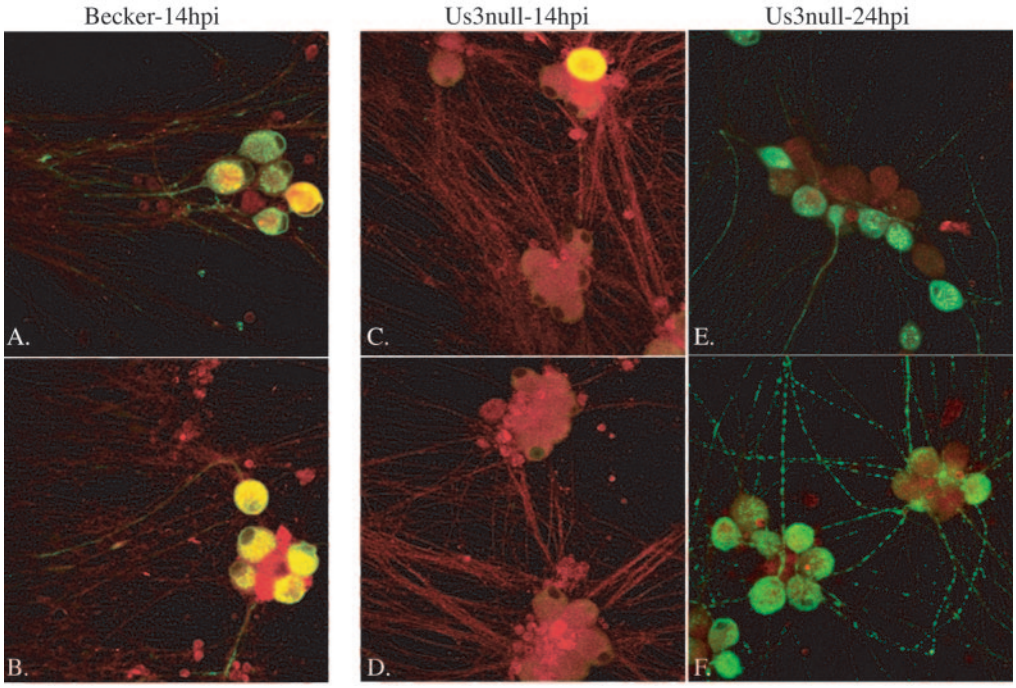

FIG. 8. Analysis of axon-mediated infection of cell bodies. Infection was initiated in the N compartment and followed for 14 or 24 h. At these times, cells were fixed with 2% paraformaldehyde and stained with the lipid marker DiI (red) to mark all neuronal membranes and with antibodies specific for gE (green). PRV Becker (A and B)- and PRV 813 (Us3 null) (C and D)-infected cells are shown at 14 h postinfection (pi). PRV 813 (Us3 null)-infected cells are shown at 24 h pi (E and F).

death, we estimated the time to imminent death based on the onset of severe symptoms, including weight loss and behavioral eccentricities, such as uncoordinated movement, hunched posture, and labored breathing (47). Using this method, we also were able to euthanize animals, perfuse them, and isolate brain samples of high quality for further analyses. In these experiments, PRV Becker- and Us3 null revertant-infected animals exhibited severe symptoms or died by 66 h. In contrast, U_s3 null-infected animals were asymptomatic at 66 h, but they developed advanced symptoms shortly thereafter (Table 2). Animals allowed to survive beyond 66 h typically developed symptoms that became apparent approximately 70 h postinoculation and became severe within a few hours after that time. Weight loss in these animals was not as severe as that observed for PRV Becker-infected rats or Us3 null revertant-induced infections but developed rapidly over a period of hours. Weight loss is a correlate of virulence (39). These studies indicate that while Us3 null virus exhibits disease progression and pathology similar to those of PRV Becker and the Us3 null revertant, the loss of Us3 results in a modest but reproducible attenuation of virulence.

TABLE 2. Summary of virulence characteristics of PRV after ocular infection of rats

Virus	No. of animals infected	Time (h) to sacrifice (s) or death (d)	Severity of symptoms	Wt change (g)
PRV Becker	2	66 (d)	Severe	−45
		66 (s)	Severe	−33
PRV 813R	2	66 (d)	Slight	−35
		66 (s)	Moderate	−6
PRV 813	7	66 (s)	Asymptomatic	+3
		66 (s)	Asymptomatic	+12
		66 (s)	Asymptomatic	+1
		72 (s)	Slight	−11
		71 (s)	Slight	−11
		73 (s)	Severe	−9
		80 (d)	Severe	−18

Neuroinvasiveness was evaluated by examining the ability of the null mutant to invade the CNS via retinal ganglion neurons (central visual projections; anterograde) or neurons that project to various muscles and autonomic targets of the eye (retrograde). Infection of neurons in the lateral geniculate nucleus of the thalamus and superior colliculus are a reliable measure of anterograde transneuronal infection through retinal projections, whereas infection of the Edinger-Westphal nucleus results from retrograde transneuronal passage through autonomic pathways (8, 38, 40). The SCN can be infected through retinal afferents, as well as through the Edinger-Westphal nucleus. In this model, retrograde viral invasion through autonomic pathways results from the spread of virus from the vitreous body into the orbit by inadvertent leakage of inoculum through the injection site in the sclera of the eye.

Our data clearly demonstrated the capacity of the Us3 null mutant to invade the brain through both retrograde and anterograde routes. This fact is illustrated in two cases where the extent of leakage of virus into the orbit differed, as reflected by marked differences in the extents of infection of the Edinger-Westphal complex (Fig. 9 and 10). Both cases exhibited anterograde transneuronal infection of the geniculate nucleus and tectum at approximately 70 h, consistent with anterograde

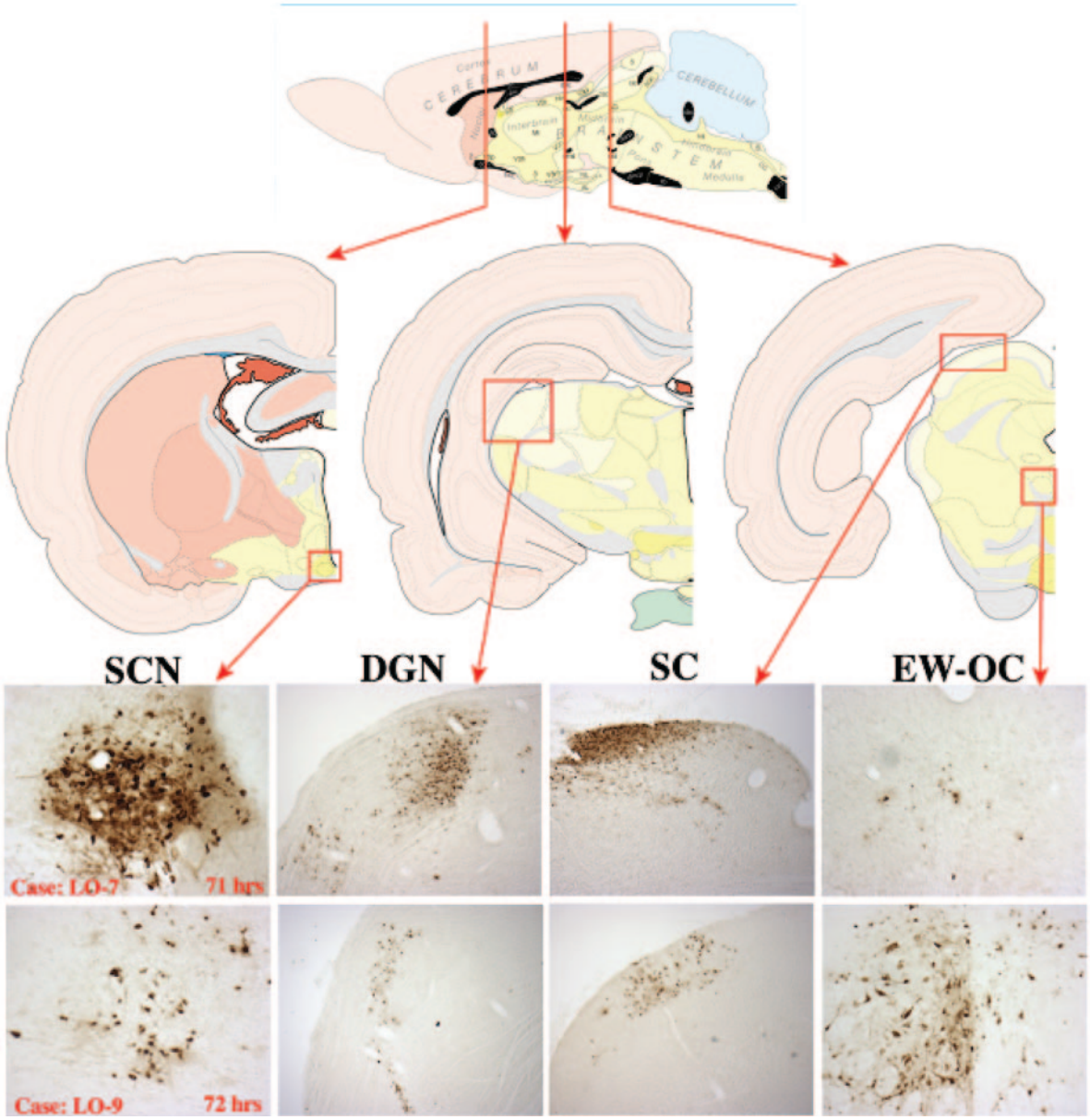

FIG. 9. Neuroinvasion of PRV 813 (Us3 null) in two cases: LO-7 and LO-9. Retrograde and anterograde circuits of the intraocular-infection model are shown (top): retrograde, Edinger Westphal/oculomotor nucleus (EW-OC) and SCN; anterograde, superior coliculus (SC) and dorsal geniculate nucleus (DGN). Brain sections were stained for PRV antigen using polyvalent antisera produced against inactivated purified PRV virions. Shown are case LO-7 at 71 h and case LO-9 at 72 h after infection.

transneuronal infection via retinal ganglion cells. However, the magnitudes of infection in these regions differed substantially. In case LO-7, infection of the geniculate nucleus and tectum was dense at 71 h. Additionally, the SCN in this case, which also receives input from retinal ganglion cells, was densely infected in spite of the fact that the Edinger-Westphal nucleus was sparsely infected. These data differed from case LO-9, where infection of the geniculate nucleus, tectum, and SCN at 72 h was of lesser magnitude and viral spread through autonomic pathways was clearly indicated by a robust infection of the Edinger-Westphal nucleus. The dense infection of the SCN in case LO-7 in the absence of spread of virus through autonomic pathways is consistent with the presence of retinal ganglion cells projecting directly to this hypothalamic nucleus. The number of retinal ganglion cells projecting into the SCN is substantially less than that of ganglion cells that project into the geniculate and tectum. We interpret the data from this case as follows: reduced leakage of virus to the orbit resulted in higher concentrations of virus in the vitreous body available to infect the retinal ganglion cells. The high concentration of inoculum in the vitreous body enabled infection of the sparse retinal ganglion cell population that projects into the SCN. This explanation is also consistent with the pattern of infection observed in case LO-9. There, the substantial infection of neu-

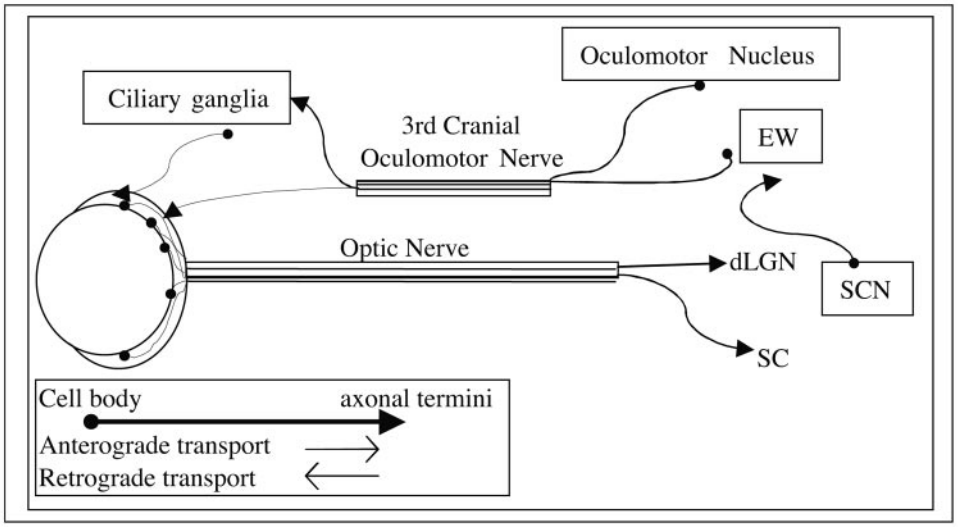

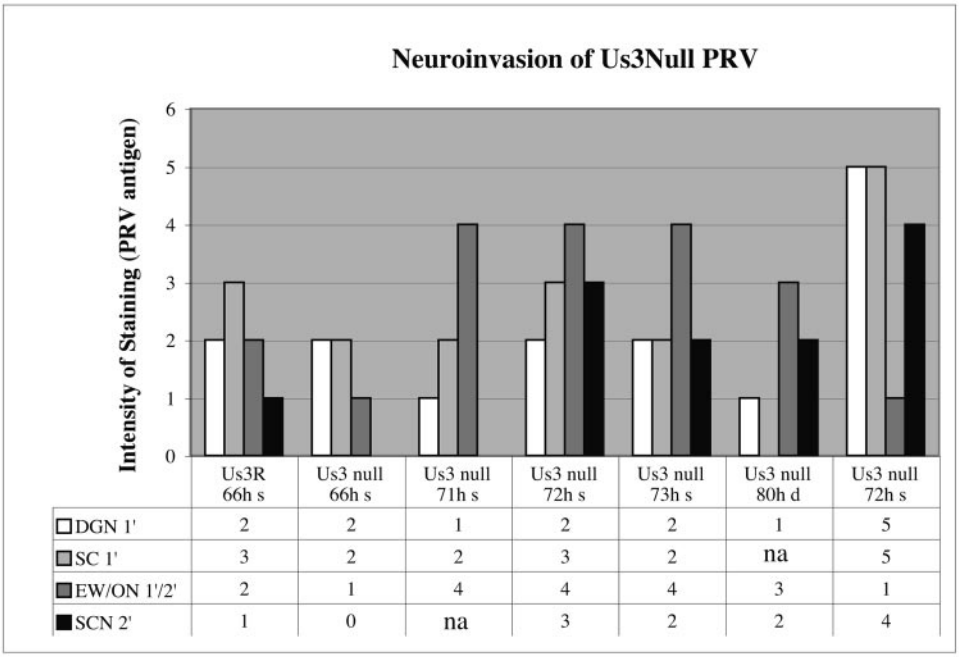

	Us3R 66h s	Us3 null 66h s	Us3 null 71h s	Us3 null 72h s	Us3 null 73h s	Us3 null 80h d	Us3 null 72h s
DGN 1'	2	2	1	2	2	1	5
SC 1'	3	2	2	3	2	na	5
EW/ON 1'/2'	2	1	4	4	4	3	1
SCN 2'	1	0	na	3	2	2	4

FIG. 10. PRV neuroinvasion of the CNS. (Top) Schematic diagram of some of the neural circuitry associated with the eye. (Bottom) Animals were perfused at the time of death (d) or sacrifice (s). The hours postinfection are indicated. Brain sections were ranked according to increasing levels of PRV antigen (range, 1 [low] to 5 [high]) by visual inspection. Spread of PRV 813R (Us3R) and PRV 813 (Us3 null) to primary (1′) and secondary (2′) synaptically connected neurons in the anterograde and retrograde visual circuits can be seen both numerically and visually in the bar graph.

rons in the Edinger-Westphal nucleus was indicative of more virus inoculum leakage into the eye orbit, which in turn resulted in reduced infection of retinal ganglion cells and then of neurons in the geniculate nucleus and tectum. Additionally, the extent of infection in the SCN reflected multisynaptic retrograde transneuronal infection through autonomic pathways at this survival interval. Collectively, these data demonstrate that the Us3 null mutant can infect neural circuitry by both retrograde and anterograde transneuronal routes and that the temporal progression of infection through both pathways is dependent on the concentration of virus at the site of infection.

Kinetics of retrograde transport in axons. We observed a reduction in viral antigen in distal CNS nuclei after Us3 null mutant infection, as well as a reduction in the number of infected cell bodies in the trichamber compartment system. A possible explanation for these results could be that the efficiency of retrograde transport of Us3 null mutant capsids on microtubules within axons is reduced after infection. To examine this possibility, we infected SCG explant cultures for 30 min at 37°C with PRV 180 (red capsid) and PRV 823 (red capsid/Us3 null mutant) to facilitate live imaging of capsids of entering viral particles. Infected cultures were transferred to a heated chamber assembly (Live Cell Systems) for imaging using a Perkin-Elmer spinning-disc confocal microscope. The movements of mRFP-VP26-tagged fluorescent capsids were tracked using Imageview (Perkin-Elmer). Qualitatively, Us3

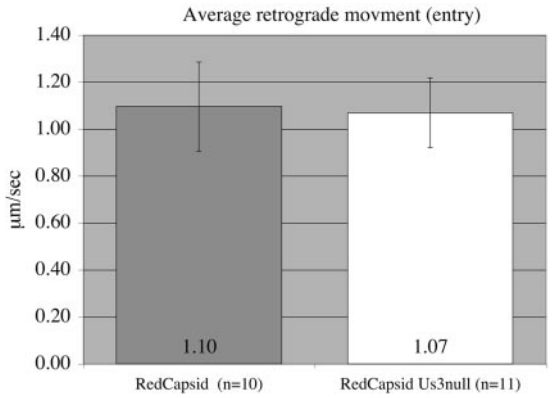

FIG. 11. Average particle velocities during axon-mediated infection. The average velocity of particles (fluorescent puncta) in axons after entry was determined using live microscopy on explants of superior cervical ganglia infected with fluorescently tagged viruses that express or do not express Us3. Entering capsids exhibited similar retrograde transport kinetics in the presence (RedCapsid) or absence (RedCapsid-Us3null) of Us3.

null red puncta exhibited similar dynamics and no increase or decrease in stalls or bidirectional movement compared to PRV 180 particles. The average capsid velocity for PRV 180 was 1.1 ± 0.19 μm/s, while the average velocity for PRV 823 capsids was 1.07 ± 0.15 μm/s. The difference between these two data sets was not statistically significant (Fig. 11). These values are also similar to previously documented dynamics for capsids tagged with eGFP-VP26 undergoing retrograde transport in cultured chick sensory neurons (1.17 ± 0.03 μm/s) (43). Interestingly, we observed in multiple samples that fewer Us3 null particles were moving compared to similarly prepared PRV 180-infected samples. While further work is needed to substantiate these initial observations, Us3 null mutants do appear to exhibit a delay in events early after entry. These defects could explain, in part, the appearance of reduced viral antigens in cell bodies observed in vitro and in vivo for Us3 null infections.

DISCUSSION

Although Us3 is unique to and universally conserved among the neurotropic alphaherpesviruses, its absence from the PRV genome has modest to no obvious effect on the replication and spread of infection in PC12 cells and in cultured PNS neurons. In animals, Us3 null mutants are capable of spreading to and infecting CNS neurons either by efferent or afferent routes. However, Us3 null mutants do have a distinct virulence phenotype in animals in that infected animals develop symptoms later and live longer than wild-type-infected animals. The precise mechanism for the reduced-virulence phenotype is likely to reflect both the 10-fold replication defect of Us3 null virus observed in PC12 cells and primary neuronal cultures and the delayed infection of autonomic circuits by retrograde routes. Studies of cultured neurons also indicated that Us3 null mutants may have a delay in early axonal entry events. This initial delay could be sufficient to retard subsequent replication in cell bodies, which in turn would slow subsequent propagation to presynaptic cells.

The presence of Us3 in the tegument, as well as its association with the capsid during transport to the nucleus, places it in a prime position to modulate entry events (23). Us3 could affect general processes at entry, such as tegument uncoating or processes leading to capsid association with microtubule motors. Tegument uncoating has been related to the phosphorylation activity of the PRV-encoded serine/threonine protein kinase UL13 (36). Perhaps phosphorylation of virion components is required for efficient dispersal of capsid and tegument to allow efficient retrograde transport to the nucleus. Alternatively, modification of cellular elements, such as actin or other cytoskeletal elements, may be required for short-range transport or other processes necessary for immediate movement away from surface membranes and subsequent cargo loading of motor proteins (41). These processes could be specific to axons or terminus regions of the neuron or may be a general aspect of entry. In any event, delays in entry will be exacerbated by the long-distance transport of capsids to the cell body, a process inherent in retrograde infection of neuronal termini. Interestingly, the attenuated Bartha strain of PRV has several mutations in Us3 that result in the absence or partial inefficiency of virion packaging of Us3 (22, 32). PRV Bartha is an excellent tracer of neuronal circuitry, as the attenuated virulence allows extensive spread in chains of connected neurons within the brains of infected animals. However, PRV Bartha is restricted for anterograde spread and is a retrograde-only tracer (38, 40). Recent studies have suggested that PRV Bartha also exhibits a modest delay in axon-mediated infection of neuronal cell bodies (53).

ACKNOWLEDGMENTS

We thank members of the Enquist laboratory for advice, reagents, and discussion. In particular, the comments and suggestions of Alex Flood were invaluable. We thank Bruce Banfield and Greg Smith for providing unpublished information. Trisha Barney and Marlies Eldridge provided invaluable technical support. Joe Goodhouse provided expert assistance in confocal microscopy.

This work was supported by NIH grant R01-NS33506 to L.W.E.

REFERENCES

1. **Asano, S., T. Honda, F. Goshima, Y. Nishiyama, and Y. Sigiura.** 2000. Us3 protein kinase of herpes simplex virus protects primary afferent neurons from virus-induced apoptosis in ICR mice. Neurosci. Lett. **294:**105–108.
2. **Banfield, B. W., J. D. Kaufman, J. A. Randall, and G. E. Pickard.** 2003. Development of pseudorabies virus strains expressing red fluorescent proteins: new tools for multisynaptic labeling applications. J. Virol. **77:**10106–10112.
3. **Banfield, B. W., G. S. Yap, A. C. Knapp, and L. W. Enquist.** 1998. A chicken embryo eye model for the analysis of alphaherpesvirus neuronal spread and virulence. J. Virol. **72:**4580–4588.
4. **Bartha, A.** 1961. Experimental reduction of virulence of Aujeszky's disease virus. Magy. Allat. Lapja **16:**42–45.
5. **Brittle, E. E., A. E. Reynolds, and L. W. Enquist.** 2004. Two modes of pseudorabies virus neuroinvasion and lethality in mice. J. Virol. **78:**12951–12963.
6. **Calton, C. M., J. A. Randall, M. W. Adkins, and B. W. Banfield.** 2004. The pseudorabies virus serine/threonine kinase Us3 contains mitochondrial, nuclear and membrane localization signals. Virus Genes **29:**131–145.
7. **Card, J. P., M. E. Whealy, A. K. Robbins, and L. W. Enquist.** 1992. Pseudorabies virus envelope glycoprotein gI influences both neurotropism and virulence during infection of the rat visual system. J. Virol. **66:**3032–3041.
8. **Card, J. P., M. E. Whealy, A. K. Robbins, R. Y. Moore, and L. W. Enquist.** 1991. Two alpha herpesvirus strains are transported differentially in the rodent visual system. Neuron **6:**957–969.
9. **Ch'ng, T.-H., E. A. Flood, and L. W. Enquist.** 2004. Culturing primary and transformed neuronal cells for studying pseudorabies virus infection. Humana Press, Totowa, N.J.
10. **Ch'ng, T. H., and L. W. Enquist.** 2005. Efficient axonal localization of alphaherpesvirus structural proteins in cultured sympathetic neurons requires viral glycoprotein E. J. Virol. **79:**8835–8846.
11. **Ch'ng, T. H., and L. W. Enquist.** 2005. Neuron-to-cell spread of pseudorabies virus in a compartmented neuronal culture system. J. Virol. **79:**10875–10889.

12. **del Rio, T., T. H. Ch'ng, E. A. Flood, S. P. Gross, and L. W. Enquist.** 2005. Heterogeneity of a fluorescent tegument component in single pseudorabies virus virions and enveloped axonal assemblies. J. Virol. **79:**3903–3919.
13. **Demmin, G. L., A. C. Clase, J. A. Randall, L. W. Enquist, and B. W. Banfield.** 2001. Insertions in the gG gene of pseudorabies virus reduce expression of the upstream Us3 protein and inhibit cell-to-cell spread of virus infection. J. Virol. **75:**10856–10869.
14. **de Wind, N., A. Zijderveld, K. Glazenburg, A. Gielkens, and A. Berns.** 1990. Linker insertion mutagenesis of herpesviruses: inactivation of single genes within the Us region of pseudorabies virus. J. Virol. **64:**4691–4696.
15. **Dohner, K., A. Wolfstein, U. Prank, C. Echeverri, D. Dujardin, R. Vallee, and B. Sodiek.** 2002. Function of dynein and dynactin in herpes simplex virus capsid transport. Mol. Biol. Cell **13:**2795–2809.
16. **Dohner, K., C.-H. Nagel, and B. Sodiek.** 2005. Viral stop-and-go along microtubules: taking a ride with dynein and kinesins. Trends Microbiol. **13:**320–327.
17. **Enquist, L. W., and J. P. Card.** 2003. Recent advances in the use of neurotropic viruses for circuit analysis. Curr. Opin. Neurobiol. **13:**603–606.
18. **Enquist, L. W., P. J. Husak, B. W. Banfield, and G. A. Smith.** 1998. Infection and spread of alpha herpesviruses in the nervous system. Adv. Virus Res. **58:**237–347.
19. **Enquist, L. W., M. J. Tomishima, S. Gross, and G. A. Smith.** 2002. Directional spread of an alpha herpesvirus in the nervous system. Vet. Microbiol. **86:**5–16.
20. **Geenen, K., H. W. Favoreel, and H. J. Nauwynck.** 2005. Higher resistance of porcine trigeminal ganglion neurons towards pseudorabies virus-induced cell death compared with other porcine cell types in vitro. J. Gen. Virol. **86:** 1251–1260.
21. **Geenen, K., H. W. Favoreel, L. Olsen, L. W. Enquist, and H. J. Nauwynck.** 2004. The pseudorabies virus Us3 protein kinase possesses anti-apoptotic activity that protects cells from apoptosis during infection and after treatment with sorbitol or staurosporine. Virology **331:**144–150.
22. **Granzow, H., B. G. Klupp, and T. C. Mettenleiter.** 2004. The pseudorabies virus Us3 protein is a component of primary and of mature virions. J. Virol. **78:**1314–1323.
23. **Granzow, H., B. G. Klupp, and T. C. Mettenleiter.** 2005. Entry of pseudorabies virus: an immunogold-labeling study. J. Virol. **79:**3200–3205.
24. **Greene, L. A., S. E. Farinelli, M. E. Cunningham, and D. S. Park.** 1998. Culture and experimental use of PC12 rat pheochromocytoma cell line, p. 161–187. *In* G. Banker and K. Goslin (ed.), Culturing nerve cells, 2nd ed. MIT Press, Cambridge, Mass.
25. **Klopfleisch, R., J. P. Teifke, W. Fuchs, M. Kopp, B. G. Klupp, and T. C. Mettenleiter.** 2004. Influence of tegument proteins of pseudorabies virus on neuroinvasion and transneuronal spread in the nervous system of adult mice after intranasal inoculation. J. Virol. **78:**2956–2966.
26. **Kurachi, R., T. Daikoku, T. Tsurumi, K. Maeno, Y. Nishiyama, and T. Kurata.** 1993. The pathogenicity of a Us3 protein kinase-deficient mutant of herpes simplex virus type 2 in mice. Arch. Virol. **133:**259–273.
27. **Kuypers, H., and G. Ugolini.** 1990. Viruses as transneuronal tracers. Trends Neurosci. **13:**71–75.
28. **LaVail, J. H., A. N. Tauscher, J. W. Hicks, O. Harrabi, G. T. Melrose, and D. M. Knipe.** 2005. Genetic and molecular in vivo analysis of herpes simplex virus assembly in murine visual system neurons. J. Virol. **79:**11142–11150.
29. **Lomniczi, B., S. Watanabe, T. Ben-Porat, and A. S. Kaplan.** 1987. Genome location and identification of functions defective in the Bartha vaccine strain of pseudorabies virus. J. Virol. **61:**796–801.
30. **Luxton, G. W., S. Haverlock, K. E. Coller, S. E. Antinone, A. Pincetic, and G. A. Smith.** 2005. Targeting of herpesvirus capsid transport in axons is coupled to association with specific sets of tegument proteins. Proc. Natl. Acad. Sci. USA **102:**5832–5837.
31. **Luxton, G. W., J. I. Lee, S. Haverlock-Moyns, J. M. Schober, and G. A. Smith.** 2006. The pseudorabies virus VP1/2 tegument protein is required for intracellular capsid transport. J. Virol. **80:**201–209.
32. **Lyman, M. G., G. L. Demmin, and B. W. Banfield.** 2003. The attenuated pseudorabies virus strain Bartha fails to package the tegument proteins Us3 and VP22. J. Virol. **77:**1403–1414.
33. **Meignier, B., R. Longnecker, P. Mavromara-Nazos, A. E. Sears, and B. Roizman.** 1988. Virulence of and establishment of latency by genetically engineered deletion mutants of herpes simplex virus I. Virology **162:**251–254.
34. **Mettenleiter, T. C.** 2000. Aujeszky's disease (pseudorabies) virus: the virus and molecular pathogenesis—state of the art, June 1999. Vet. Res. **31:**99–115.
35. **Mettenleiter, T. C.** 1996. Immunobiology of pseudorabies (Aujeszky's disease). Vet. Immunol. Immunopathol. **54:**221–229.
36. **Morrison, E. E., Y.-F. Wang, and D. M. Meridith.** 1998. Phosphorylation of structural components promotes dissociation of the herpes simplex virus type 1 tegument. J. Virol. **72:**7108–7114.
37. **Nishiyama, Y., Y. Yamada, R. Kurachi, and T. Daikoku.** 1992. Construction of a Us3 *lacZ* insertion mutant of herpes simplex virus type 2 and characterization of its phenotype in vitro and in vivo. Virology **190:**256–268.
38. **Pickard, G. E., C. A. Smeraski, C. C. Tomlinson, B. W. Banfield, J. Kaufman, C. L. Wilcox, L. W. Enquist, and P. J. Sollars.** 2002. Intravitreal injection of the attenuated pseudorabies virus PRV Bartha results in infection of the hamster suprachiasmatic nucleus only by retrograde transsynaptic transport via autonomic circuits. J. Neurosci. **22:**2701–2710.
39. **Pomeranz, L. E., A. E. Reynolds, and C. J. Hengartner.** 2005. Molecular biology of pseudorabies virus: impact on neurovirology and veterinary medicine. Microbiol. Mol. Biol. Rev. **69:**462–500.
40. **Smeraski, C. A., P. J. Sollars, M. D. Ogilvie, L. W. Enquist, and G. E. Pickard.** 2004. Suprachiasmatic nucleus input to autonomic circuits identified by retrograde transsynaptic transport of pseudorabies virus from the eye. J. Comp. Neurol. **471:**298–313.
41. **Smith, G. A., and L. W. Enquist.** 2002. Break ins and break outs: viral interactions with the cytoskeleton of mammalian cells. Annu. Rev. Cell Dev. Biol. **18:**135–161.
42. **Smith, G. A., and L. W. Enquist.** 2000. A self-recombining bacterial artificial chromosome and its application for analysis of herpesvirus pathogenesis. Proc. Natl. Acad. Sci. USA **97:**4873–4878.
43. **Smith, G. A., L. Pomeranz, S. P. Gross, and L. W. Enquist.** 2004. Local modulation of plus-end transport targets herpesvirus entry and egress in sensory axons. Proc. Natl. Acad. Sci. USA **101:**16034–16039.
44. **Sodeik, B.** 2000. Mechanisms of viral transport in the cytoplasm. Trends Microbiol. **8:**465–472.
45. **Sodeik, B., M. W. Ebersold, and A. Helenius.** 1997. Microtubule-mediated transport of incoming herpes simplex virus 1 capsids to the nucleus. J. Cell Biol. **136:**1007–1021.
46. **Strack, A. M., and A. D. Loewy.** 1990. Pseudorabies virus: a highly specific transneuronal cell body marker in the sympathetic nervous system. J. Neurosci. **10:**2139–2147.
47. **Tirabassi, R. S., and L. W. Enquist.** 2000. Role of the pseudorabies virus gI cytoplasmic domain in neuroinvasion, virulence, and posttranslational N-linked glycosylation. J. Virol. **74:**3505–3516.
48. **Tomishima, M. J., and L. W. Enquist.** 2001. A conserved alpha-herpesvirus protein necessary for axonal localization of viral membrane proteins. J. Cell Biol. **154:**741–752.
49. **Wagenaar, F., J. M. A. Pol, B. Peters, A. L. J. Gielkens, N. deWind, and T. G. Kimman.** 1995. The Us3-encoded protein kinase from pseudorabies virus affects egress of virions from the nucleus. J. Gen. Virol. **76:**1851–1859.
50. **Whealy, M. E., J. P. Card, A. K. Robbins, J. R. Dubin, H. J. Rziha, and L. W. Enquist.** 1993. Specific pseudorabies virus infection of the rat visual system requires both gI and gp63 glycoproteins. J. Virol. **67:**3786–3797.
51. **Wittmann, G., and H. J. Rziha.** 1989. Aujeszky's disease (pseudorabies) in pigs, p. 230–333. *In* G. Wittmann (ed.), Herpesvirus diseases of cattle, horse and pigs. Kluwer Academic, Boston, Mass.
52. **Wolfstein, A., C.-H. Nagel, K. Radtke, K. Dohner, V. J. Allan, and B. Sodeik.** 2006. The inner tegument promotes herpes simplex virus capsid motility along microtubules in vitro. Traffic **7:**227–237.
53. **Yang, M., J. P. Card, R. S. Tirabassi, R. R. Miselis, and L. W. Enquist.** 1999. Retrograde, transneuronal spread of pseudorabies virus in defined neuronal circuitry of the rat brain is facilitated by gE mutations that reduce virulence. J. Virol. **73:**4350–4359.